

Fanning and Bending Sub-Voxel Structures in Diffusion MRI

S. Nedjati-Gilani¹, and D. C. Alexander¹

¹Centre for Medical Image Computing, University College London, London, United Kingdom

Introduction We present a new model for fanning and bending white matter structures on a sub-voxel scale, and explore the suitability of the model for estimating the degree of fanning in each voxel of a human brain diffusion MRI acquisition. This method allows us to quantify the degree of fanning and bending directly.

Method We devise a parametric model of how the fibre orientation varies spatially over the voxel in fanning and bending structures. Figure 1 illustrates the concepts used for the model. We divide each voxel into a sub-voxel grid. The fanning or bending structure of the sub-voxels is determined by the position of the voxel grid relative to the centre of a series of concentric circles. For fanning structures, the orientation at each sub-voxel is determined by the radial line passing through the centre of the sub-voxel. The closer the grid is to the centre, the greater the degree of fanning. Changing the position of the grid relative to the centre affects the orientation of the fanning structure, as sub-voxel grids (a) and (b) of Figure 1 demonstrate. Grid (c) shows how the orientations change when the position of the grid is altered. Using tangential, rather than radial directions to define the sub-voxel fibre orientations, models bending in a similar way. To control the fanning and bending structure for all sub-voxels s_i in voxel l , we define the parameter set $\mathbf{p}(l) = \{a, r, \mathbf{u}, \psi\}$, where r controls the distance of the voxel grid relative to the centre of the circles, a controls the anisotropy of the fanning by allowing the ratio of the sub-voxel dimensions to vary, and \mathbf{u} and ψ control the position of the grid relative to the centre of the circles. For each sub-voxel, we assume Behrens' ball and stick model [1] with one fibre population so that for sub-voxel s and wavenumbers $\mathbf{q}_k, k=1\dots M$, we have measurements $A(s, \mathbf{q}_k) = (1-f) \exp(-t|\mathbf{q}_k|^2 d) + f \exp(-td(\mathbf{e}_s \cdot \mathbf{q}_k)^2)$, where f is the volume fraction, \mathbf{e} is the orientation of the fibre population, d is the diffusivity and t is the diffusion time. We take f and d to be constant for all sub-voxels in the grid, and fit the model to the data by minimizing $E(l) = \sum_{k=1}^M (A(l, \mathbf{q}_k) - \tilde{A}(l, \mathbf{q}_k))^2$ directly with a Levenberg-Marquardt algorithm to find $\mathbf{p}(l)$, where $A(l, \mathbf{q}_k)$ are the voxel measurements, and $\tilde{A}(l, \mathbf{q}_k)$ are the measurements reconstructed by summing sub-voxel measurements over the sub-voxel grid. The sub-voxel measurements are reconstructed from $\mathbf{p}(l)$ using the model. To improve the fit of the model to the measurements, we perform the minimization in several stages, minimizing $E(l)$ with respect to some of the parameters of $\mathbf{p}(l)$ whilst keeping other parameters constant at each stage of the minimization. The model requires careful initialization for the fitting procedure above to converge on sensible parameter estimates. We estimate starting positions from the fitted DT, the shape of which is sensitive to the degree and anisotropy of the fanning structure.

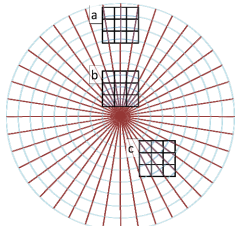


Figure 1: Illustration of the model used to create fanning structures in a sub-voxel grid. The radial line passing through the centre of each sub-voxel determines the orientation of the associated fibre population.

fraction, \mathbf{e} is the orientation of the fibre population, d is the diffusivity and t is the diffusion time. We take f and d to be constant for all sub-voxels in the grid, and fit the model to the data by minimizing $E(l) = \sum_{k=1}^M (A(l, \mathbf{q}_k) - \tilde{A}(l, \mathbf{q}_k))^2$ directly with a Levenberg-Marquardt algorithm to find $\mathbf{p}(l)$, where $A(l, \mathbf{q}_k)$ are the voxel measurements, and $\tilde{A}(l, \mathbf{q}_k)$ are the measurements reconstructed by summing sub-voxel measurements over the sub-voxel grid. The sub-voxel measurements are reconstructed from $\mathbf{p}(l)$ using the model. To improve the fit of the model to the measurements, we perform the minimization in several stages, minimizing $E(l)$ with respect to some of the parameters of $\mathbf{p}(l)$ whilst keeping other parameters constant at each stage of the minimization. The model requires careful initialization for the fitting procedure above to converge on sensible parameter estimates. We estimate starting positions from the fitted DT, the shape of which is sensitive to the degree and anisotropy of the fanning structure.

Experiment We use the model to reconstruct fanning structure in each voxel of a region of interest containing the fanning structure in the corona radiata. We use diffusion-weighted human brain data from a $128 \times 128 \times 32$ image with 61 diffusion-weighted images with a b-value of 1200 s mm^2 and one measurement at $\mathbf{q} = \mathbf{0}$, with eight repeats of each measurement, acquired in a Philips 3T Achieva scanner. The region of interest we consider is $10 \times 14 \times 4$ voxels in size and shown in Figure 2. The ROI contains three distinct sections. The first section, highlighted in yellow in Figure 2, contains a crossing of the corona radiata with the superior longitudinal fasciculus (SLF). The section highlighted in red consists mainly of the fanning corona radiata, but may contain some crossings with fibres parallel to the SLF. In the third region, highlighted in blue, the corona radiata intersects the corpus callosum. We use our method to find fanning parameters for each voxel in the ROI, and assume each voxel consists of a $5 \times 5 \times 5$ sub-voxel grid.

Results Figure 2 shows the resulting fibre population distributions in a sagittal slice of the ROI, and compares the results of the new method (Figure 2d) to those obtained from fitting the diffusion tensor (Figure 2b) and using PAS-MRI [2] (Figure 2c). In the case of the diffusion tensor reconstruction, the results show the 'mean' orientation of the fanning structure in each voxel, but the DT cannot distinguish between a single anisotropic fibre population in a voxel, and a more complex fanning structure. Results from PAS-MRI suggest fanning structures in these voxels in a qualitative manner, but interpreting the results to obtain quantitative information about the degree of fanning is a non-trivial task. The peaks of the PAS reconstructions are anisotropic in this region [3], which suggests fanning qualitatively, but it is difficult to determine the precise degree of fanning from the peak shape [3]. PAS suggests two-fibre crossings in some fanning areas. Although possible, the crossings are likely to be spurious in lower regions of the ROI, and more likely to be correct higher up where the SLF intersects in the red ROI. The new method suggests plausible fanning structures for voxels where we expect fanning, although we can see that in a minority of voxels (such as the voxel highlighted in green in Figure 2d), the optimization process visibly fails to find the global minimum, resulting in unlikely fanning distributions given the distributions of neighbouring voxels.

Conclusions and Future Work We have presented a model for generating fanning structures on a sub-voxel scale. Preliminary work suggests that we can use the model to reconstruct fanning structures in real brain data and provide quantitative information about the fanning structure. Defining the structure more accurately allows more appropriate action to be taken by tractography algorithms, resulting in fewer false positive and false negative tracts. Further work will include an algorithm that uses fanning and bending models to the voxel measurements to classify voxels as either containing a fanning or bending structure. Such an algorithm will require knowledge from neighbouring voxels, as in [4]; if the set of sub-voxel orientations produced by fanning and bending models are the same, the spatial arrangement of the orientations will not affect the sum of the sub-voxel measurements.

References [1] Behrens et al, *MRM* 2003;50:1077-1088 [2] Jansons and Alexander, *Inverse Problems*; 2004;19:1031-146 [3] Seunarine et al, *ISMRM* 2008;1831; [4] Savadjiev et al, *NeuroImage* 2008;41:58-68.

Acknowledgements This research was conducted with the aid of funding by Philips Medical Systems and EPSRC. We would like to acknowledge G. J. M. Parker for providing the human brain data used in this work.

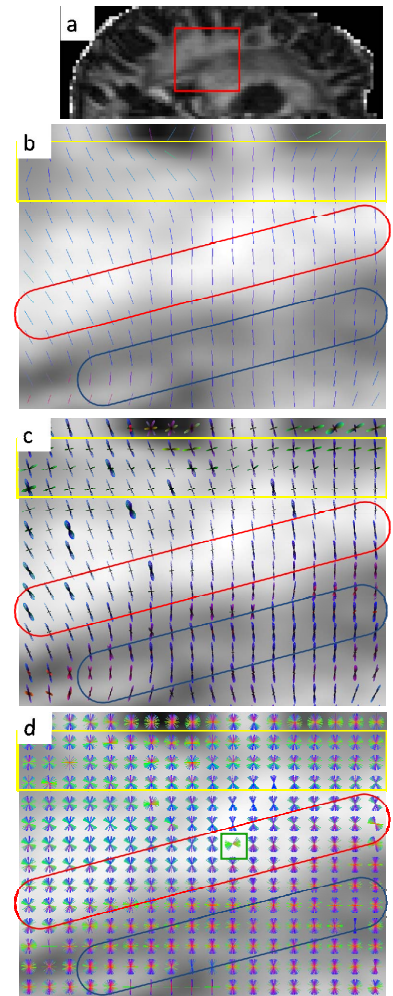


Figure 2: (a) FA map with the corona radiata highlighted and reconstructions from (b) DT (c) PAS-MRI and (d) sub-voxel fanning model, showing the fanning distribution in each voxel.